Doping dependence of polaron hopping energies in $La_{1-x}Ca_xMnO_3$ $(0 \leq x \leq 0.15)$

K. P. Neupane,[1] J. L. Cohn,[1] H. Terashita,[2,*] and J. J. Neumeier[2]
[1]*Department of Physics, University of Miami, Coral Gables, Florida 33124, USA*
[2]*Department of Physics, Montana State University, Bozeman, Montana 59717, USA*
(Received 6 April 2006; revised manuscript received 3 August 2006; published 27 October 2006)

Measurements of the low-frequency ($f \leq 100$ kHz) permittivity at $T \leq 160$ K and dc resistivity ($T \leq 430$ K) are reported for $La_{1-x}Ca_xMnO_3$ $(0 \leq x \leq 0.15)$. Static dielectric constants are determined from the low-T limiting behavior of the permittivity. The estimated polarizability for bound holes $\sim 10^{-22}$ cm^{-3} implies a radius comparable to the interatomic spacing, consistent with the small polaron picture established from prior transport studies near room temperature and above on nearby compositions. Relaxation peaks in the dielectric loss associated with charge-carrier hopping yield activation energies in good agreement with low-T hopping energies determined from variable-range hopping fits of the dc resistivity. The doping dependence of these energies suggests that the orthorhombic, canted antiferromagnetic ground state tends toward an insulator-metal transition that is not realized due to the formation of the ferromagnetic insulating state near Mn^{4+} concentration ≈ 0.13.

DOI: 10.1103/PhysRevB.74.144428 PACS number(s): 75.47.Lx, 75.50.Ee, 77.22.Ch, 77.22.Gm

I. INTRODUCTION

The Mn^{3+}-rich insulating compounds, $La_{1-x}A_xMnO_3$ (A = Sr, Ca, $x \leq 0.15$) have attracted considerable interest in recent years for their inhomogeneous magnetic ground states,[1] and complex structural phase diagrams,[2,3] believed to be consequences of competing magnetic, lattice, and Coulomb interactions.[4] With regard to transport properties, there is general consensus that the charge-carriers in the high-T paramagnetic phases of these compounds are small polarons.[5–7] However, few systematic studies of the doping dependence of polaron transport in the insulating regime have been reported.[8] The experimental situation is complicated by the sensitivity of the structural and magnetic properties to deviations in stoichiometry[2,3] and the uncertain stoichiometry of specimens employed in many early transport studies.

Here we present dielectric and dc resistivity measurements on a series of $La_{1-x}Ca_xMnO_3$ polycrystalline specimens with $x \leq 0.15$ that offer insight into the role of electron correlations on the changes in ground state magnetic and crystal structure that occur[1–3] near Mn^{4+} content, $p = p_c \simeq 0.13$. Consistent with the small-polaron picture, the doping dependence of the dielectric constant yields a bound-polaron polarizability that implies a localization length comparable to a lattice spacing. In agreement with prior work[8] on $La_{1-x}Sr_xMnO_3$ we find that the high-temperature polaron hopping energy is independent of p up to p_c, above which it begins to decrease. Particularly interesting are low-temperature measurements of dielectric relaxation and dc resistivity which indicate a polaron hopping energy that tends toward zero near p_c. These results suggest that charge carriers within the orthorhombic, canted antiferromagnetic (CAF) phase are approaching an insulator-metal transition that is not achieved due to the emergence of the monoclinic and ferromagnetic insulating (FMI) phase.

II. EXPERIMENT

Polycrystalline specimens of $La_{1-x}Ca_xMnO_{3+\delta}$ were prepared by standard solid-state reaction under Ar atmosphere; the preparation methods, structural characterization, and magnetic properties are reported elsewhere.[9] Powder x-ray diffraction revealed no secondary phases; the average Mn^{4+} (hole) concentration ($p = x + 2\delta$) was determined by iodometric titration (see Table I). A small and nearly x-independent oxygen excess ($\delta_{av} \approx 0.017$) in the present specimens is attributed to cation vacancies[10,11] which contribute additional holes uniformly,[11] similar to Ca substitution. The structural and magnetic properties of the present specimens are consistent with those of stoichiometric compounds.[3,11]

Alternating current impedance measurements were conducted with an HP4263B LCR meter at frequencies f = 100 Hz, 120 Hz, 10 kHz, 20 kHz, 100 kHz using a 4-terminal pair arrangement. Reliable measurements of ε were restricted to $T \leq 160$ K where the capacitive reactance was sufficiently large ($\gtrsim 0.1\ \Omega$). Typical specimen dimensions were $3 \times 1.0 \times 0.5$ mm^3. Silver paint electrodes were applied on the largest, polished faces of the specimens. Contact capacitance can lead to apparently large values[12] of ε and thus some care is required to distinguish the true response of the sample. To rule out the influence of contacts, the impedances of several specimens were remeasured after further polishing to reduce the electrode spacing by at least a factor of 2; in all cases the low-temperature data used to determine ε_0 agreed within geometric uncertainties of ±10%. The results were also independent of applied ac voltage in the range 50 mV–1 V. At higher temperatures where dielectric relaxation was observed, some dependence on the electrode spacing was evident, consistent with a contribution from contact capacitance. This issue is addressed further below. Four-probe dc resistivity measurements were performed in separate experiments in air (high T) and vacuum (low T) with current applied along the long axis of the same specimens used for ac impedance.

III. RESULTS AND ANALYSIS

Quite generally, the complex dielectric permittivity of a solid, $\varepsilon = \varepsilon' - i\varepsilon''$, can be expressed as $\varepsilon = \varepsilon_\infty + \varepsilon_l + \varepsilon_d$. ε_∞ is the

 ©2006 The American Physical Society

TABLE I. Nominal Ca and measured Mn^{4+} concentrations, dielectric constant, activation energies (E_δ), and prefactors (ω_0) of Arrhenius relaxation rates determined from tan δ, and $T_0^{1/4}$ and $E_{\rho/T}$ determined from the dc resistivities for $La_{1-x}Ca_xMnO_3$ specimens.

x	$p \equiv Mn^{+4}$ (%)	ε_0	E_δ (meV)	ω_0 (s^{-1})	$T_0^{1/4}$ ($K^{1/4}$)	$E_{\rho/T}$ (meV)
0.00	4.0	17.6	125	1.49×10^{11}	–	–
0.02	5.7	11.3	202	2.03×10^{13}	234	231
0.04	7.8	12.7	182	3.26×10^{12}	228	232
0.06	9.9	11.7	155	1.09×10^{12}	208	233
0.08	11.3	13.8	126	1.42×10^{11}	185	233
0.10	12.6	16.3	65.5	2.58×10^{9}	155	233
0.12	14.1	17.8	43.9	4.42×10^{9}	148	220
0.14	17.4	21.4	37.9	1.05×10^{10}	134	209
0.15	–	20.9	26.8	5.21×10^{8}	–	–

high-frequency dielectric constant associated with displacements of ionic charge distributions relative to their nuclei. The lattice contribution, ε_l, arises from displacements of ions and their charge distributions. ε_d represents a dipolar contribution, associated in the present materials with charge-carrier hopping as discussed below. ε_∞ and ε_l are generally frequency and temperature independent at low T.

Figure 1 shows $\varepsilon'(T)$ at four frequencies for five Ca concentrations in the low-T regime where ε' becomes frequency and temperature independent. The intrinsic static dielectric constant $\varepsilon_0 \equiv \varepsilon'(T \to 0)$ can be determined directly from the data. The sharp increase of $\varepsilon'(\omega)$ and onset of frequency dispersion with increasing temperature, signatures of dielectric relaxation, are more clearly manifested in the broader temperature range of Fig. 2 (for $x=0.08$) as steps in ε' and maxima in the loss factor, $\tan\delta \equiv \varepsilon''/\varepsilon'$.

A significant feature of the relaxation behavior for all specimens is that the temperatures of the maxima in tan δ (denoted T_{max}) and inflections in $\varepsilon'(T)$ differ substantially (dashed lines in Fig. 2). This rules out an intrinsic dipole response, for which these features occur at the same temperature.[13,14] Schottky barriers are to be expected at metal-semiconductor contacts with manganites.[12,15] The associated depletion layers behave as a large capacitance in parallel with a resistor, in series with the bulk specimen. Assuming that the contact capacitance is nearly temperature independent, the time constant of the system (τ) is controlled by the temperature-dependent bulk resistance of the specimen,[12] with maxima in $\tan\delta$ occurring for $\omega\tau \simeq 1$. Consistent with this picture, Freitas *et al.*[15] have demonstrated for a related manganite compound that large values of ε' (at $T \geq 150$ K in Fig. 2) are sensitive to the type of contacts employed (e.g., silver paint, vapor-deposited metals), but that the charge-carrier activation energies derived from the $\tan\delta$ maxima are contact independent.

Figure 3 shows a semilog plot of ω vs $100/T_{max}$ for several specimens, demonstrating Arrhenius behavior for the relaxation rates, $\tau^{-1}(T) = \omega_0 \exp(-E_\delta/k_B T)$. Values of E_δ and ω_0 were determined from the slopes and intercepts, respectively, of linear-least-squares fits (solid lines, Fig. 3) and are listed in Table I.

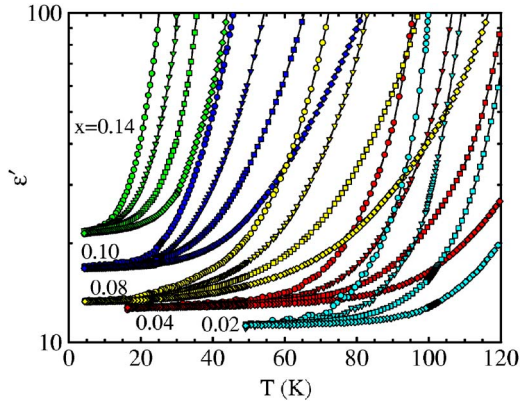

FIG. 1. (Color online) ε' vs T for $La_{1-x}Ca_xMnO_3$ specimens at frequencies 100 Hz, 1 kHz, 10 kHz, 100 kHz (increasing from left to right for each composition).

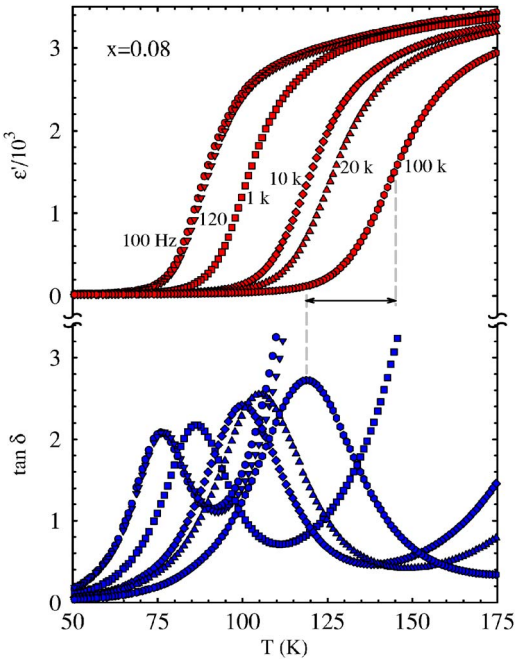

FIG. 2. (Color online) ε' and loss tangent vs T at different frequencies for $x=0.08$.

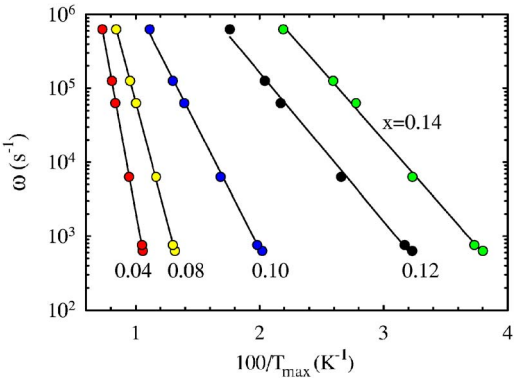

FIG. 3. (Color online) ω vs $100/T_{max}$ for several Ca concentrations. Solid lines are linear-least-squares fits.

Figure 4 shows dc resistivity measurements for the same specimens. The low-T data ($T \leq 160$ K) in Fig. 4(a) are plotted against $T^{-1/4}$, suggesting the variable-range hopping form,[16] $\rho = \rho_0 \exp[-(T_0/T)^{1/4}]$. The $T^{-1/2}$ Efros-Shklovskii[17] hopping form is equally satisfactory over the limited temperature range of the linear-least-squares fits (solid lines). High-T resistivity data (240 K $\leq T \leq$ 440 K) in Fig. 4(b) are shown plotted to emphasize the adiabatic small-polaron form widely established for the paramagnetic phase of these materials,[5–8] $\rho/T = A \exp(E_{\rho/T}/k_B T)$. Solid lines are linear-least-squares fits used to determine $E_{\rho/T}$; these values and those for $T_0^{1/4}$ are listed in Table I. The Jahn-Teller (JT) structural transition is clearly evidenced by a vertical displacement of the data for $x=0.12$ [arrow in Fig. 4(b)] over a broad temperature interval over which the lattice constants are observed to change.[3] The slopes above and below the transition are the same, in agreement with similar studies of $La_{1-x}Sr_xMnO_3$.[8] A transition for the $x=0.06$ specimen is also evident, but is not completed at the maximum temperature investigated. The JT transition for the $x=0.14$ specimen is expected somewhat below room temperature;[3] the absence of a noticeable feature in $\rho(T)$ is consistent with the systematic broadening and eventual disappearance of features in structural and magnetic measurements with increased doping near this hole concentration.[3]

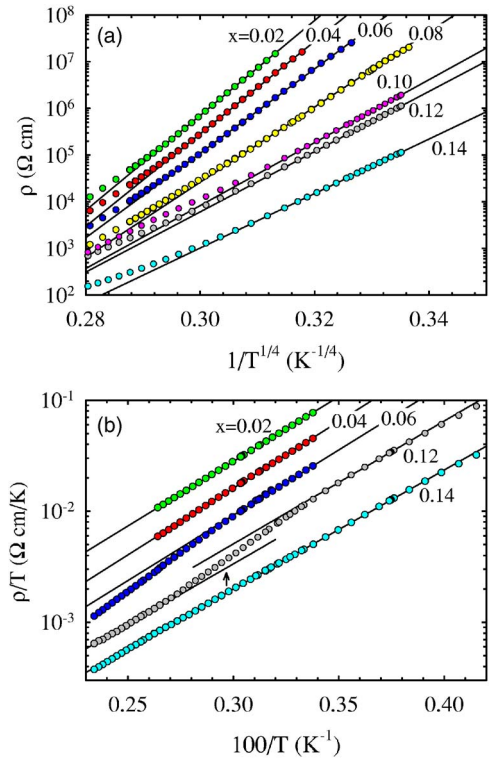

FIG. 4. (Color online) (a) ρ vs $1/T^{1/4}$ at low temperatures for $La_{1-x}Ca_xMnO_3$, (b) high-temperature data plotted in the adiabatic small-polaron form. Data for $x=0.08$ and 0.10 are omitted for clarity in (b). Solid lines in both figures are linear-least-squares fits.

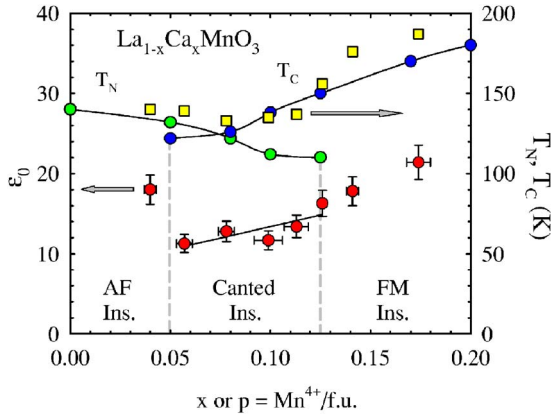

FIG. 5. (Color online) ε_0 vs Mn^{4+} concentration from the present study (left ordinate). The solid line is a linear-least-squares fit to the data for $0.057 \leq p \leq 0.126$. Also shown are data for T_N and T_C (right ordinate) determined from magnetization measurements on polycrystalline specimens from the same batch as those used here for dielectric measurements (squares, Ref. 9), and from neutron diffraction on single crystals (circles, Ref. 1). The vertical dashed lines delineate approximate low-T magnetic phase boundaries from Ref. 1.

IV. DISCUSSION

The dependence of ε_0 on the hole concentration, p, is shown in Fig. 5. For the nominally undoped compound[18] $LaMnO_3$, $\varepsilon_0 = 18$. A smaller value, $\varepsilon_0 \approx 12$, is observed for $p \sim 0.05-0.10$, and an approximately linear increase for $p \geq 0.10$. Also shown are the magnetic phase boundaries defined by T_N or T_C from magnetization data on polycrystals from the same batches as those reported here[9] (squares and right ordinate, Fig. 5) and neutron diffraction studies of single crystals[1] (circles and right ordinate, Fig. 5). The recently clarified structural phase diagram[3] indicates orthorhombic and monoclinic structures for the CAF and FMI regimes, respectively, with a transition occurring in the range $0.12 \leq p \leq 0.14$.

Let us first consider the decrease in ε_0 at the lowest hole concentrations. This behavior is contrary to expectations based on the behavior of conventional semiconductors[19] where the dielectric constant of the (undoped) host lattice ($\varepsilon_{0,h}$) is enhanced at low temperatures by the presence of electrons or holes bound to donor or acceptor impurities,

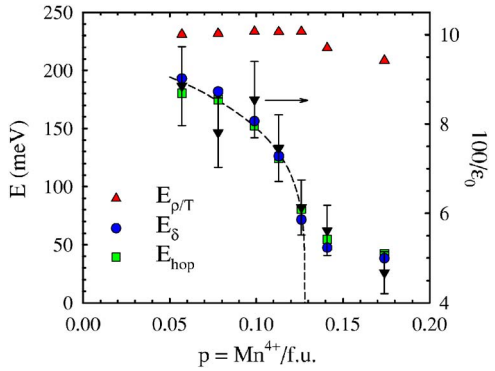

FIG. 6. (Color online) Activation energies (left ordinate) determined from dielectric relaxation (E_δ) and dc resistivities at high T ($E_{\rho/T}$) and low T (E_{hop}), and inverse dielectric constant (right ordinate) vs Mn^{4+} concentration.

respectively. Local fields produced by charged defects, La and Mn vacancies, and excess oxygen,[10,11] can influence the polarizability associated with bound holes in the ground state. The observed decrease in ε_0 by $\sim$30% would require a corresponding decrease in the acceptor polarizability due to differences in the long-range magnetic and/or orbital structure of the A-type AF and CAF states.

The increase of ε_0 for $p \geq 0.05$ is consistent with a growing contribution from holes bound to acceptors in the present materials (Ca or excess oxygen). An estimate of the polarizability can be found from the solid line in Fig. 5 using the dilute limit of the Castellan-Seitz[20] expression, $\varepsilon_0 - \varepsilon_{0,h} = 4\pi N \alpha_0$, where $N \equiv p/V_{fu}$ is the acceptor density and V_{fu} is the volume per formula unit.[9] This yields $\alpha_0 \simeq 2.8 \times 10^{-22}$ cm^3 which implies (for hydrogenic impurities) a Bohr radius $a_H = (2\alpha_0/9\varepsilon_{0,h})^{1/3} \simeq 1.7$ Å (we take $\varepsilon_{0,h} = 12$ from Fig. 5 as representative of the CAF phase). Thus the ε_0 data imply electronic states for the bound holes that are localized at individual atomic sites, consistent with general consensus from transport studies near room temperature and above, that doped holes move as small polarons.[5–7]

It is instructive to examine and compare the various polaron energies determined from our measurements. As noted above, we expect E_δ to represent the low-T charge-carrier hopping energy. Supporting this conclusion, we find excellent agreement between E_δ and the hopping energy determined from the dc resistivity variable-range hopping fits,[16] $E_{hop} = 0.25 k_B T_0^{1/4} T^{3/4}$, where T in this expression was taken as the average T_{max} for each composition. Figure 6 shows these energies as a function of doping. Also plotted is the high-T polaron activation energy, $E_{\rho/T}$, which remains approximately constant at $\sim$230 meV up to $p_c \approx 0.13$. At higher doping it decreases, a trend quite similar to that reported for $La_{1-x}Sr_xMnO_3$.[8] Most striking is the behavior of E_{hop} which appears to be dropping sharply toward zero at p_c, and exhibits a clear change in doping dependence for $p > p_c$. The dashed curve in Fig. 6 is an empirical power-law fit, $E_{hop} = 220(1 - p/0.128)^{1/4}$. The inverse dielectric constant, also shown (right ordinate, Fig. 6), appears to follow a very similar behavior.

$E_{hop}(p)$ is reminiscent of the behavior of conventional doped semiconductors[21] near the insulator-metal transition (IMT), with p_c the critical density. This point of view is encouraged by the observation that p_c and a_H are close to satisfying the Mott criterion[22] for an IMT, $N_c^{1/3} a_H \simeq 0.26 \pm 0.05$. Experimentally we find $\approx$0.22. Thus the data suggest that the ground-state structural and magnetic transitions[1,3] occurring near p_c are a consequence of the rapidly growing charge-carrier kinetic energy as $p \rightarrow p_c$ within the orthorhombic, CAF phase. The change in orbital-ordering scheme in the monoclinic, FMI phase[3] might be viewed as a compromise among competing magnetic, lattice, and Coulomb energies that suppresses the rate of growth in kinetic energy with doping, and "delays" the IMT to higher Mn^{4+} concentration. Given this low-T picture of proximity to an IMT, it is natural to hypothesize that the decrease in the high-T small-polaron energy, $E_{\rho/T}$, at $p > p_c$ reflects the cooperative effects of overlapping polarons.

Scaling behavior is to be expected near the IMT, with physical properties controlled by a localization length diverging as $\xi = \xi_0 (1 - p/p_c)^{-\nu}$, with ν a critical exponent. With[16] $T_0 \propto 1/\xi^3$, this yields $T_0^{1/4} \propto (1 - p/p_c)^{3\nu/4}$, and our empirical fit (dashed curve, Fig. 6) implies $\nu \simeq 1/3$. Though smaller than values in the range $1/2 \leq \nu \leq 1$ that have been reported for doped Si and Ge,[21,23] this estimate of ν should be viewed with caution as a lower bound since the scaling theory applies only very close to p_c where the present data are not sufficiently dense. Furthermore, the inhomogeneous ground state of these materials may alter scaling behavior. This is especially likely near p_c where both orthorhombic and monoclinic domains may coexist[3] and where the coalescence of ferromagnetic clusters of nanoscopic size embedded in the CAF matrix have been deduced from neutron scattering studies.[1]

In summary, combined dielectric and resistivity measurements reveal new systematics of electronic degrees of freedom in the complex magnetic and structural phase behavior of lightly doped $La_{1-x}Ca_xMnO_3$. The doping dependence of the dielectric constant and low-T hopping energies suggest that adding holes within the CAF ground state drives the electronic system toward an insulator-metal transition near Mn^{4+} concentration $\approx$0.13. That this transition is not realized is evidently a manifestation of competition from magnetic and lattice energies reflected in the emergence of the FMI phase.

ACKNOWLEDGMENTS

The authors acknowledge experimental assistance from C. Chiorescu. This material is based upon work supported by the National Science Foundation under Grants No. DMR-0072276 (Univ. Miami) and No. DMR-0504769 (Montana State Univ.), and from the Research Corporation (Univ. Miami).

*Present address: Research Center Jülich, D-52425 Jülich, Germany.

[1] G. Biotteau, M. Hennion, F. Moussa, J. Rodr'iguez-Carvajal, L. Pinsard, A. Revcolevschi, Y. M. Mukovskii, and D. Shulyatev, Phys. Rev. B **64**, 104421 (2001); M. Hennion, F. Moussa, G. Biotteau, J. Rodríguez-Carvajal, L. Pinsard, and A. Revcolevschi, Phys. Rev. Lett. **81**, 1957 (1998).

[2] A. Urushibara, Y. Moritomo, T. Arima, A. Asamitsu, G. Kido, and Y. Tokura, Phys. Rev. B **51**, 14103 (1995); H. Kawano, R. Kajimoto, M. Kubota, and H. Yoshizawa, *ibid.* **53**, R14709 (1996); B. Dabrowski, X. Xiong, Z. Bukowski, R. Dybzinski, P. W. Klamut, J. E. Siewenie, O. Chmaissem, J. Shaffer, C. W. Kimball, J. D. Jorgensen, and S. Short, *ibid.* **60**, 7006 (1999).

[3] M. Pissas, I. Margiolaki, G. Papavassiliou, D. Stamopoulos, and D. Argyriou, Phys. Rev. B **72**, 064425 (2005).

[4] E. Dagotto, T. Hotta, and A. Moreo, Phys. Rep. **344**, 1 (2001); E. Dagotto, *Nanoscale Phase Separation and Colossal Magneto-Resistance,* Springer Series in Solid-State Sciences Vol. 136 (Springer-Verlag, Berlin, 2003).

[5] M. Jaime, H. T. Hardner, M. B. Salamon, M. Rubinstein, P. Dorsey, and D. Emin, Phys. Rev. Lett. **78**, 951 (1997).

[6] J. M. De Teresa, K. Dörr, K. H. Müller, L. Schultz, and R. I. Chakalova, Phys. Rev. B **58**, R5928 (1998).

[7] J. L. Cohn, J. Supercond. **13**, 291 (2000).

[8] P. Mandal, B. Bandyopadhyay, and B. Ghosh, Phys. Rev. B **64**, 180405(R) (2001).

[9] H. Terashita and J. J. Neumeier, Phys. Rev. B **71**, 134402 (2005).

[10] J. A. M. van Roosmalen and E. H. P. Cordfunke, J. Solid State Chem. **110**, 109 (1994).

[11] B. Dabrowski, R. Dybzinski, Z. Bukowski, O. Chmaissem, and J. D. Jorgensen, J. Solid State Chem. **146**, 448 (1999).

[12] P. Lunkenheimer, V. Bobnar, A. V. Pronin, A. I. Ritus, A. A. Volkov, and A. Loidl, Phys. Rev. B **66**, 052105 (2002).

[13] J. Volger, in *Progress in Semiconductors*, edited by A. F. Gibson (Wiley, New York, 1960), Vol. 4, p. 207, and references therein.

[14] R. K. Grubbs, E. L. Venturini, P. G. Clem, J. J. Richardson, B. A. Tuttle, and G. A. Samara, Phys. Rev. B **72**, 104111 (2005).

[15] R. S. Freitas, J. F. Mitchell, and P. Schiffer, Phys. Rev. B **72**, 144429 (2005).

[16] N. F. Mott and E. A. Davis, *Electronic Processes in Noncrystalline Materials*, 2nd ed. (Clarendon, Oxford, 1979).

[17] A. L. Efros and B. I. Shklovskii, J. Phys. C **8**, L49 (1975).

[18] J. L. Cohn, M. Peterca, and J. J. Neumeier, Phys. Rev. B **70**, 214433 (2004).

[19] T. G. Castner, N. K. Lee, G. S. Cieloszyk, and G. L. Salinger, Phys. Rev. Lett. **34**, 1627 (1975); H. F. Hess, K. DeConde, T. F. Rosenbaum, and G. A. Thomas, Phys. Rev. B **25**, 5578 (1980).

[20] C. W. Castellan and F. Seitz, *Semiconducting Materials*, edited by H. K. Henisch (Butterworths, London, 1951).

[21] W. N. Shafarman and T. G. Castner, Phys. Rev. B **33**, 3570 (1986).

[22] N. F. Mott, Can. J. Phys. **34**, 1356 (1956); P. P. Edwards and M. J. Sienko, Phys. Rev. B **17**, 2575 (1976).

[23] H. F. Hess, K. DeConde, T. F. Rosenbaum, and G. A. Thomas, Phys. Rev. B **25**, 5578 (1982); M. A. Paalanen, T. F. Rosenbaum, G. A. Thomas, and R. N. Bhatt, Phys. Rev. Lett. **48**, 1284 (1982); G. A. Thomas, Y. Ootuka, S. Katsumoto, S. Kobayashi, and W. Sasaki, Phys. Rev. B **25**, 4288 (1982).